# Hexagonal QMF Banks and Wavelets

*A chapter within Time-Frequency and Wavelet Transforms in Biomedical Engineering,*
*M. Akay (Editor), New York, NY: IEEE Press, 1997.*

Sergio Schuler and Andrew Laine

Computer and Information Science and Engineering Department

University of Florida

Gainesville, FL 32611

# Hexagonal QMF Banks and Wavelets

Sergio Schuler and Andrew Laine

Department of Computer and Information Science and Engineering

University of Florida

Gainesville, FL 32611

## INTRODUCTION

In this chapter we shall lay bare the theory and implementation details of hexagonal sampling systems and hexagonal quadrature mirror filters (HQMF). Hexagonal sampling systems are of particular interest because they exhibit the tightest packing of all regular two-dimensional sampling systems and for a circularly band-limited waveform, hexagonal sampling requires 13.4 percent fewer samples than rectangular sampling [1]. In addition, hexagonal sampling systems also lead to nonseparable quadrature mirror filters in which all basis functions are localized in space, spatial frequency and orientation [2]. This chapter is organized in two sections. Section I describes the theoretical aspects of hexagonal sampling systems while Section II covers important implementation details.

## I. HEXAGONAL SAMPLING SYSTEM

This section presents the theoretical foundation of hexagonal sampling systems and hexagonal quadrature mirror filters. Most of this material has appeared elsewhere in [1], [3], [4], [5], [2], [6] but is described here under a unified notation for completeness. In addition, it will provide continuity and a foundation for the original material that follows in Section II. The rest of the section is organized as follows. Section I-A covers the general formulation of a hexagonal sampling system. Section I-B introduces up-sampling and down-sampling in hexagonal sampling systems. Section I-C reviews the theory of hexagonal quadrature mirror filters. Section I-D describes redundant analysis/synthesis filter banks in hexagonal systems. Finally, Section I-E covers the formulation of the discrete Fourier transform in hexagonal sampling systems.

*A. Hexagonal systems*

Let $x_a(\mathbf{t}) = x_a(t_1, t_2)$ be a 2-D analog waveform, then a sampling operation in 2-D can be represented by a lattice formed by taking all integer linear combinations of a set of two linearly independent vectors $\mathbf{v}_1 = [v_{11}\ v_{21}]^{\mathrm{T}}$ and $\mathbf{v}_2 = [v_{12}\ v_{22}]^{\mathrm{T}}$. Using vector notation we can represent the lattice as the set of all vectors $\mathbf{t} = [t_1\ t_2]^{\mathrm{T}}$ generated by

$$\mathbf{t} = \mathbf{V}\mathbf{n}, \tag{1}$$

where $\mathbf{n} = [n_1\ n_2]^{\mathrm{T}}$ is an integer-valued vector and $\mathbf{V} = [\mathbf{v}_1\ \mathbf{v}_2]$ is a $2 \times 2$ matrix, known as the *sampling matrix*. Because $\mathbf{v}_1$ and $\mathbf{v}_2$ are chosen to be linearly independent, the determinant of $\mathbf{V}$ is nonzero. Note that $\mathbf{V}$ is not unique for a given sampling pattern and that two matrices representing the same sampling process are related by a linear transformation represented by a unimodular matrix [7].

Sampling an analog signal $x_a(\mathbf{t})$ on the lattice defined by (1) produces the discrete signal

$$x(\mathbf{n}) = x_a(\mathbf{V}\mathbf{n}).$$

Figure 1(a) shows a hexagonal sampling lattice defined by the pair of sampling vectors

$$\mathbf{v}_1 = \begin{bmatrix} 2T_1 \\ 0 \end{bmatrix} \text{ and } \mathbf{v}_2 = \begin{bmatrix} -T_1 \\ T_2 \end{bmatrix}, \tag{2}$$

where $T_1 = \frac{1}{2}$ and $T_2 = \frac{\sqrt{3}}{2}$. The lattice is hexagonal since each sample location has exactly six nearest neighbors when $T_2 = T_1\sqrt{3}$.

Let the Fourier transform of $x_a(\mathbf{t})$ be defined by

$$X_a(\mathbf{\Omega}) = \int_{-\infty}^{+\infty} x_a(\mathbf{t}) \exp(-j\mathbf{\Omega}^{\mathrm{T}}\mathbf{t}) d\mathbf{t},$$

where $\mathbf{\Omega} = [\Omega_1\ \Omega_2]^{\mathrm{T}}$. Similarly, let the Fourier transform of the sequence $x(\mathbf{n})$ be defined as

$$X(\boldsymbol{\omega}) = \sum_{\mathbf{n}} x(\mathbf{n}) \exp(-j\boldsymbol{\omega}^{\mathrm{T}}\mathbf{n}), \tag{3}$$

where $\boldsymbol{\omega} = [\omega_1\ \omega_2]^{\mathrm{T}}$. Mersereau [4] showed that the spectrum of the sequence $x(\mathbf{n})$ and the spectrum of the signal $x_a(\mathbf{t})$ are related by

$$X(\boldsymbol{\omega}) = \frac{1}{|\det \mathbf{V}|} \sum_{\mathbf{k}} X_a(\mathbf{V}^{-\mathrm{T}}(\boldsymbol{\omega} - 2\pi\mathbf{k})), \tag{4}$$
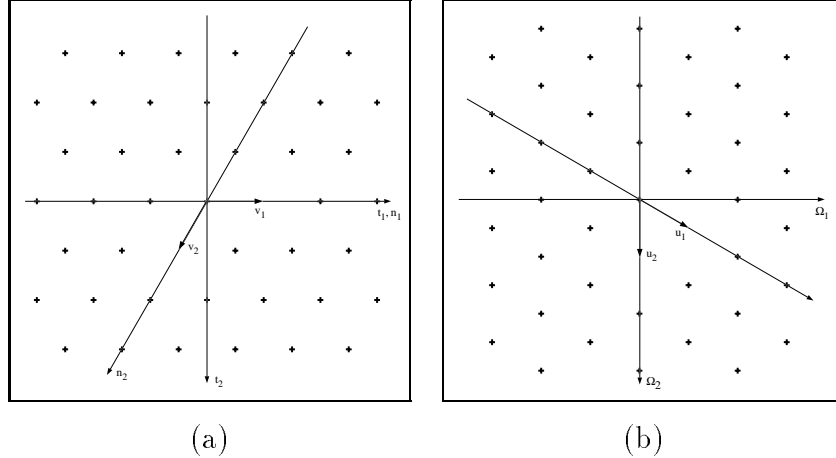
(a)          (b)

Fig. 1. (a) A hexagonal sampling lattice in the spatial domain. (b) Hexagonal sampling lattice in the frequency domain.

where $\mathbf{k}$ is an integer-valued vector and $\mathbf{V}^{-\mathrm{T}}$ denotes $(\mathbf{V}^{-1})^{\mathrm{T}}$.

Alternatively, we can define the Fourier transform of the sequence $x(\mathbf{n})$ as

$$
\begin{aligned}
X_{\mathrm{V}}(\mathbf{\Omega}) &= \sum_{\mathbf{n}} x(\mathbf{n}) \exp(-j\mathbf{\Omega}^{\mathrm{T}}\mathbf{V}\mathbf{n}) \\
&= X(\mathbf{V}^{\mathrm{T}}\mathbf{\Omega}),
\end{aligned}
\tag{5}
$$

then Equation (4) may be written as

$$
X_{\mathrm{V}}(\mathbf{\Omega}) = \frac{1}{|\det \mathbf{V}|} \sum_{\mathbf{k}} X_a(\mathbf{\Omega} - \mathbf{U}\mathbf{k}),
\tag{6}
$$

where

$$
\mathbf{U} = 2\pi\mathbf{V}^{-\mathrm{T}}.
\tag{7}
$$

Thus, Equation (6) can be interpreted as a periodic extension of $X_a(\mathbf{\Omega})$ with periodicity vectors $\mathbf{u}_1 = [u_{11}\ u_{21}]^{\mathrm{T}}$ and $\mathbf{u}_2 = [u_{12}\ u_{22}]^{\mathrm{T}}$, where $\mathbf{U} = [\mathbf{u}_1\ \mathbf{u}_2]$. The set of all vectors $\mathbf{\Omega}$ generated by $\mathbf{\Omega} = \mathbf{U}\mathbf{n}$ defines a lattice in the frequency domain known as the modulation or reciprocal lattice. Thus, the spectrum of a sequence $x(\mathbf{n})$ can be viewed as the convolution of the spectrum of $x_a(\mathbf{t})$ with a modulation lattice defined by $\mathbf{U}$.

Figure 1(b) shows the reciprocal lattice corresponding to the sampling vectors defined in Equation (2), that is the lattice defined by the pair of modulation vectors

$$
\mathbf{u}_1 = \begin{bmatrix} \frac{\pi}{T_1} \\ \frac{\pi}{T_2} \end{bmatrix} \text{ and } \mathbf{u}_2 = \begin{bmatrix} 0 \\ \frac{2\pi}{T_2} \end{bmatrix}.
$$

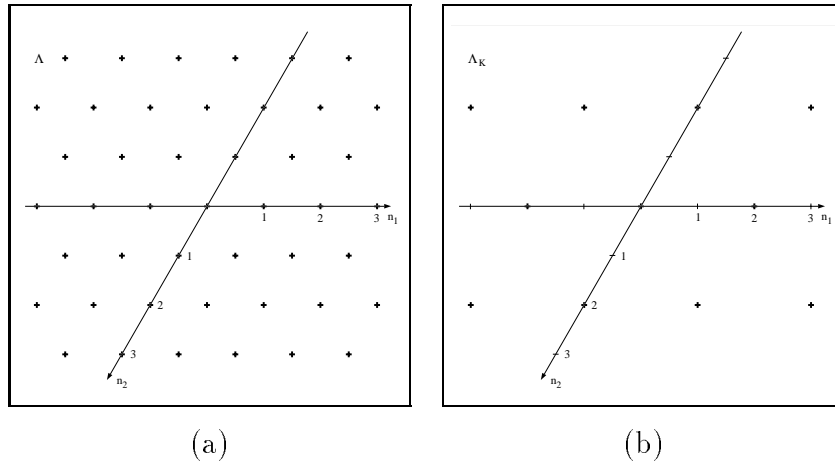Fig. 2. (a) Integer sampling lattice. (b) Sampling sublattice.

## B. Up-sampling and down-sampling in hexagonal systems

Let $\Lambda$ denote the integer lattice defined by the set of integer vectors $\mathbf{n}$, and let $\Lambda_{\mathrm{K}}$ denote the sampling sublattice generated by the subsampling matrix $\mathbf{K}$, that is the set of integer vectors $\mathbf{m}$ such that $\mathbf{m} = \mathbf{Kn}$. Note that in order to properly define a sublattice of $\Lambda$, a subsampling matrix must be nonsingular with integer-valued entries. In general, a sublattice of $\Lambda$ is called separable if it can be represented by a diagonal matrix $\mathbf{K}$, otherwise it is called nonseparable. Figure 2 shows an integer sampling lattice $\Lambda$ and a sampling sublattice $\Lambda_{\mathrm{K}}$, for the separable subsampling matrix

$$\mathbf{K} = \begin{bmatrix} 2 & 0 \\ 0 & 2 \end{bmatrix}. \tag{8}$$

With $\Lambda$ and $\Lambda_{\mathrm{K}}$ defined in this way, we can view the operations of up-sampling and down-sampling as described below.

The process of up-sampling maps a signal on $\Lambda$ to a new signal that is nonzero only at points on the sampling sublattice $\Lambda_{\mathrm{K}}$. The output of an up-sampler is related to the input by

$$y(\mathbf{n}) = \begin{cases} x(\mathbf{K}^{-1}\mathbf{n}), & \text{if } \mathbf{K}^{-1}\mathbf{n} \in \Lambda, \\ 0, & \text{otherwise.} \end{cases}$$

It is easy to show [5] that the Fourier transform relates the output and input of an up-sampler by

$$Y(\boldsymbol{\omega}) = X(\mathbf{K}^{\mathrm{T}}\boldsymbol{\omega}),$$
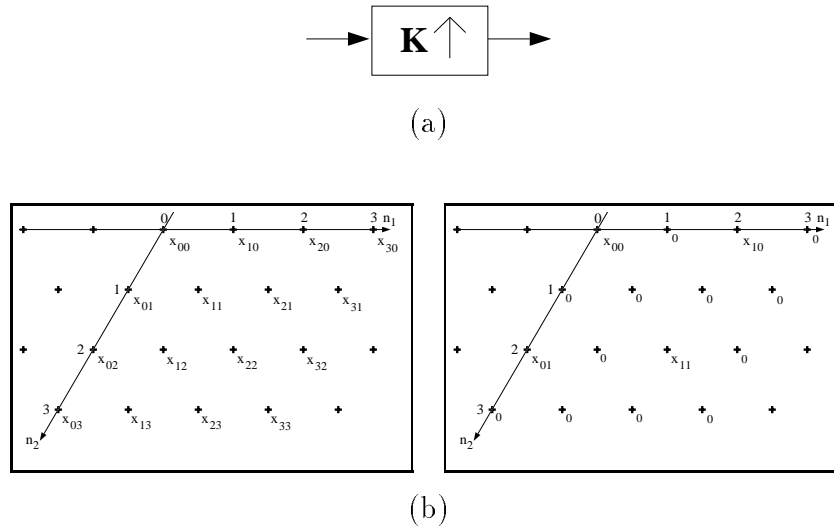
(a)



(b)

Fig. 3. (a) Up-sample operator. (b) Mapping of samples under up-sampling: (left) input signal, (right) output signal.

where $X(\boldsymbol{\omega})$ is defined by Equation (3). Figure 3 shows the block diagram of an up-sampler and the process of up-sampling for the subsampling matrix defined by Equation (8).

The process of down-sampling maps points on the sublattice $\Lambda_\text{K}$ to $\Lambda$ according to

$$y(\mathbf{n}) = x(\mathbf{Kn}), \tag{9}$$

and discards all other points.

The Fourier transform relation between the output and input of a down-sampler can be derived by introducing the concept of a sampling function $s_\text{K}(\mathbf{n})$ associated with the sampling matrix $\mathbf{K}$ [5], that is,

$$s_\text{K}(\mathbf{n}) = \begin{cases} 1, & \text{if } \mathbf{n} \in \Lambda_\text{K}, \\ 0, & \text{otherwise.} \end{cases}$$

Since $s_\text{K}(\mathbf{n})$ can be interpreted as a periodic sequence, with periodicity matrix $\mathbf{K}$, i.e. $s_\text{K}(\mathbf{n}) = s_\text{K}(\mathbf{n} + \mathbf{Km})$, it may be expressed as a Fourier series

$$s_\text{K}(\mathbf{n}) = \frac{1}{|\det \mathbf{K}|} \sum_{l=0}^{|\det \mathbf{K}|-1} \exp(-j2\pi \mathbf{k}_l^\text{T} \mathbf{K}^{-1} \mathbf{n}), \tag{10}$$

where each of the $|\det \mathbf{K}|$ vectors $\mathbf{k}_l = [k_{l_1} \ k_{l_2}]^\text{T}$ is associated with one of the cosets of $\mathbf{K}^\text{T}$. Notice that a coset of a sublattice $\Lambda_\text{K}$ is defined as the set of points obtained by shifting the entire sublattice by an integer shift vector $\mathbf{k}$. There are exactly $|\det \mathbf{K}|$ distinct cosets

of $\Lambda_K$, and their union is the integer lattice $\Lambda$. Each shift vector $\mathbf{k}_l$ associated with a certain coset is known as a coset vector. For example, one choice for the $\mathbf{k}_l$ given the sampling sublattice defined by Equation (8) is

$$\mathbf{k}_0 = \begin{bmatrix} 0 \\ 0 \end{bmatrix}, \quad \mathbf{k}_1 = \begin{bmatrix} 1 \\ 0 \end{bmatrix}, \quad \mathbf{k}_2 = \begin{bmatrix} 0 \\ 1 \end{bmatrix}, \quad \text{and} \quad \mathbf{k}_3 = \begin{bmatrix} 1 \\ 1 \end{bmatrix}. \tag{11}$$

Let

$$w(\mathbf{n}) = x(\mathbf{n})s_K(\mathbf{n}), \tag{12}$$

then it is easy to see from (9) that a down-sampled signal $y(\mathbf{n})$ can be written as

$$y(\mathbf{n}) = w(\mathbf{K}\mathbf{n}),$$

since $w(\mathbf{n})$ equals $x(\mathbf{n})$ on $\Lambda_K$. Therefore, the Fourier transform of the sequence $y(\mathbf{n})$ may be written as

$$Y(\boldsymbol{\omega}) = \sum_{\mathbf{n}} w(\mathbf{K}\mathbf{n}) \exp(-j\boldsymbol{\omega}^T\mathbf{n}). \tag{13}$$

Since $w(\mathbf{n})$ is zero for $\mathbf{n}$ not in $\Lambda_K$ we may write (13) as

$$
\begin{aligned}
Y(\boldsymbol{\omega}) &= \sum_{\mathbf{n}} w(\mathbf{n}) \exp(-j\boldsymbol{\omega}^T\mathbf{K}^{-1}\mathbf{n}) \\
&= W(\mathbf{K}^{-T}\boldsymbol{\omega}),
\end{aligned}
$$

where $W(\boldsymbol{\omega})$ is the Fourier transform of the sequence $w(\mathbf{n})$. From (10) and (12) it is easy to show that

$$W(\boldsymbol{\omega}) = \frac{1}{|\det \mathbf{K}|} \sum_{l=0}^{|\det \mathbf{K}|-1} X(\boldsymbol{\omega} + 2\pi\mathbf{K}^{-T}\mathbf{k}_l),$$

therefore, the Fourier transform relation between the output and input of a down-sampler is given by

$$Y(\boldsymbol{\omega}) = \frac{1}{|\det \mathbf{K}|} \sum_{l=0}^{|\det \mathbf{K}|-1} X(\mathbf{K}^{-T}(\boldsymbol{\omega} + 2\pi\mathbf{k}_l)).$$

Figure 4 shows the block diagram of a down-sampler and the process of down-sampling for the subsampling matrix defined on (8).

Note that the relations derived above are based on the Fourier transform defined in Equation (3). However, a more general definition is described in Equation (5). This formulation takes into account the lattice structure used to sample the original 2-D analog
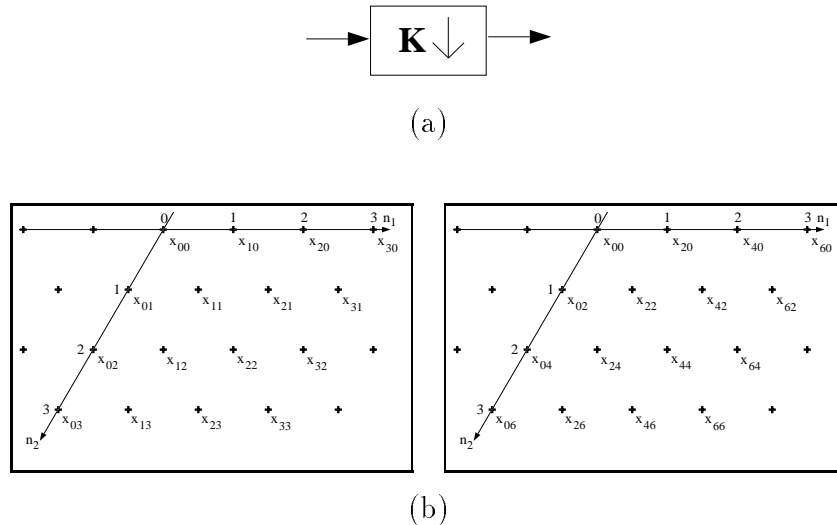
(a)



(b)

Fig. 4. (a) Down-sample operator. (b) Mapping of samples under down-sampling: (left) input signal, (right) output signal.

waveform and allows the Fourier transform relation between the input and output of an up-sampler and a down-sampler to be written as

$$Y_{\mathrm{V}}(\mathbf{\Omega}) = X(\mathbf{K}^{\mathrm{T}}\mathbf{V}^{\mathrm{T}}\mathbf{\Omega}), \qquad (14)$$

and

$$Y_{\mathrm{V}}(\mathbf{\Omega}) = \frac{1}{|\det \mathbf{K}|} \sum_{l=0}^{|\det \mathbf{K}|-1} X(\mathbf{K}^{-\mathrm{T}}(\mathbf{V}^{\mathrm{T}}\mathbf{\Omega} + 2\pi\mathbf{k}_l)). \qquad (15)$$

Therefore, if we assume $\mathbf{K}$ as defined in (8) we may write Equations (14) and (15) as

$$Y_{\mathrm{V}}(\mathbf{\Omega}) = X_{\mathrm{V}}(\mathbf{K}^{\mathrm{T}}\mathbf{\Omega}), \qquad (16)$$

and

$$Y_{\mathrm{V}}(\mathbf{\Omega}) = \frac{1}{|\det \mathbf{K}|} \sum_{l=0}^{|\det \mathbf{K}|-1} X_{\mathrm{V}}(\mathbf{K}^{-\mathrm{T}}\mathbf{\Omega} + \tilde{\mathbf{k}}_l), \qquad (17)$$

respectively, where

$$\tilde{\mathbf{k}}_l = \mathbf{U}\mathbf{K}^{-\mathrm{T}}\mathbf{k}_l. \qquad (18)$$

### C. Analysis/synthesis filter banks in hexagonal systems

This section focuses on perfect reconstruction filter banks in hexagonal sampling systems and wavelets that can be obtained by iterating such filter banks. Parts of this material are described in Simoncelli [2], but are reviewed here for completeness of presentation.
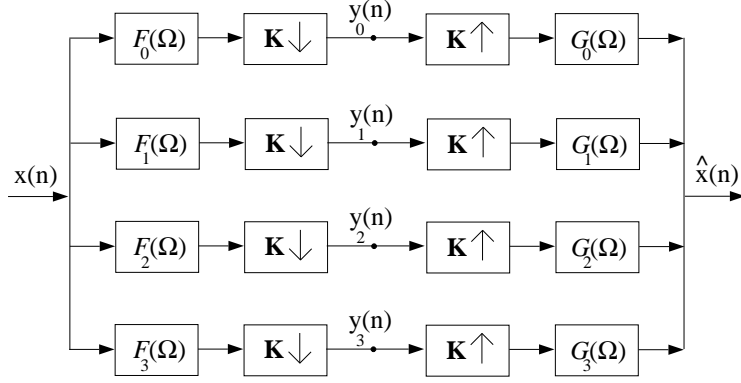
Fig. 5. A two-dimensional 4-channel analysis/synthesis filter bank.

There are a wide variety of analysis/synthesis (A/S) filter banks for two dimensional systems. We restrict our focus to analysis/synthesis filter banks in which each channel shares the same subsampling matrix $\mathbf{K}$ and the number of channels equals $|\det \mathbf{K}|$. Figure 5 shows a 4-channel analysis/synthesis filter bank. We further restrict our study to the separable sublattice defined in Equation (8) since this choice will enable us to apply the A/S filter bank recursively to each of the subband signals $y_i(\mathbf{n})$ shown in Figure 5 as described in [2].

Consider a 4-channel analysis/synthesis filter bank with $\mathbf{K}$ defined by Equation (8), then using (17) we can show that the Fourier transform of $y_i(\mathbf{n})$ may be written as

$$Y_i(\mathbf{\Omega}) = \frac{1}{|\det \mathbf{K}|} \sum_{l=0}^{|\det \mathbf{K}|-1} F_i(\mathbf{K}^{-\mathrm{T}}\mathbf{\Omega} + \tilde{\mathbf{k}}_l)X(\mathbf{K}^{-\mathrm{T}}\mathbf{\Omega} + \tilde{\mathbf{k}}_l), \tag{19}$$

where the subindex V has been suppressed for simplicity. Similarly, using (16) we have that the Fourier transform of $\hat{x}(\mathbf{n})$ is given by

$$\hat{X}(\mathbf{\Omega}) = \sum_{i=0}^{|\det \mathbf{K}|-1} G_i(\mathbf{\Omega})Y_i(\mathbf{K}^{\mathrm{T}}\mathbf{\Omega}). \tag{20}$$

Therefore, combining Equations (19) and (20) we obtain an overall filter bank response of

$$\begin{aligned}
\hat{X}(\mathbf{\Omega}) &= \frac{1}{|\det \mathbf{K}|} \sum_{i=0}^{|\det \mathbf{K}|-1} G_i(\mathbf{\Omega}) \sum_{l=0}^{|\det \mathbf{K}|-1} F_i(\mathbf{\Omega} + \tilde{\mathbf{k}}_l)X(\mathbf{\Omega} + \tilde{\mathbf{k}}_l) \\
&= \frac{1}{|\det \mathbf{K}|} \sum_{l=0}^{|\det \mathbf{K}|-1} X(\mathbf{\Omega} + \tilde{\mathbf{k}}_l) \left[ \sum_{i=0}^{|\det \mathbf{K}|-1} G_i(\mathbf{\Omega})F_i(\mathbf{\Omega} + \tilde{\mathbf{k}}_l) \right]. \tag{21}
\end{aligned}$$

Combining Equations (7), (11) and (18) for the values of $T_1$ and $T_2$ in Equation (2) yields the following set of vectors $\tilde{\mathbf{k}}_l$ , that is,

$$\tilde{\mathbf{k}}_0 = \begin{bmatrix} 0 \\ 0 \end{bmatrix}, \quad \tilde{\mathbf{k}}_1 = \begin{bmatrix} \pi \\ \frac{\pi}{\sqrt{3}} \end{bmatrix}, \quad \tilde{\mathbf{k}}_2 = \begin{bmatrix} 0 \\ \frac{2\pi}{\sqrt{3}} \end{bmatrix}, \quad \text{and} \quad \tilde{\mathbf{k}}_3 = \begin{bmatrix} \pi \\ \frac{3\pi}{\sqrt{3}} \end{bmatrix}. \tag{22}$$

From Equation (22) it is clear that one term of the sum in Equation (21) corresponds to the linear shift invariant (LSI) system response, and the remaining terms correspond to the system alias. The analysis/synthesis filter bank for which the system aliasing terms in Equation (21) are canceled is generally known as a quadrature mirror filter (QMF) bank. We can choose the filters to eliminate the aliasing terms in Equation (21) as follows

$$
\begin{aligned}
F_0(\mathbf{\Omega}) &= G_0(-\mathbf{\Omega}) &= H(\mathbf{\Omega}) = H(-\mathbf{\Omega}), \\
F_1(\mathbf{\Omega}) &= G_1(-\mathbf{\Omega}) &= \exp(j\mathbf{\Omega}^{\mathrm{T}}\mathbf{s}_1)H(\mathbf{\Omega} + \tilde{\mathbf{k}}_1), \\
F_2(\mathbf{\Omega}) &= G_2(-\mathbf{\Omega}) &= \exp(j\mathbf{\Omega}^{\mathrm{T}}\mathbf{s}_2)H(\mathbf{\Omega} + \tilde{\mathbf{k}}_2), \\
F_3(\mathbf{\Omega}) &= G_3(-\mathbf{\Omega}) &= \exp(j\mathbf{\Omega}^{\mathrm{T}}\mathbf{s}_3)H(\mathbf{\Omega} + \tilde{\mathbf{k}}_3),
\end{aligned}
\tag{23}
$$

where $\mathbf{s}_1$, $\mathbf{s}_2$ and $\mathbf{s}_3$ must satisfy the following equations

$$
\begin{aligned}
1 + e^{j\tilde{\mathbf{k}}_1^{\mathrm{T}}\mathbf{s}_1} &= 0, \quad e^{j\tilde{\mathbf{k}}_1^{\mathrm{T}}\mathbf{s}_2} + e^{j\tilde{\mathbf{k}}_1^{\mathrm{T}}\mathbf{s}_3} = 0, \\
1 + e^{j\tilde{\mathbf{k}}_2^{\mathrm{T}}\mathbf{s}_2} &= 0, \quad e^{j\tilde{\mathbf{k}}_2^{\mathrm{T}}\mathbf{s}_1} + e^{j\tilde{\mathbf{k}}_2^{\mathrm{T}}\mathbf{s}_3} = 0, \\
1 + e^{j\tilde{\mathbf{k}}_3^{\mathrm{T}}\mathbf{s}_3} &= 0, \quad e^{j\tilde{\mathbf{k}}_3^{\mathrm{T}}\mathbf{s}_1} + e^{j\tilde{\mathbf{k}}_3^{\mathrm{T}}\mathbf{s}_2} = 0.
\end{aligned}
$$

Therefore, a suitable choice for the vectors $\mathbf{s}_l$ given the vectors $\tilde{\mathbf{k}}_l$ in Equation (22) is

$$\mathbf{s}_1 = \begin{bmatrix} 1 \\ 0 \end{bmatrix}, \quad \mathbf{s}_2 = \begin{bmatrix} 1/2 \\ \sqrt{3}/2 \end{bmatrix}, \quad \text{and} \quad \mathbf{s}_3 = \begin{bmatrix} 1/2 \\ -\sqrt{3}/2 \end{bmatrix}. \tag{24}$$

After canceling all of the aliasing terms in Equation (21) the remaining LSI system response becomes

$$
\begin{aligned}
\hat{X}(\mathbf{\Omega}) &= \frac{1}{4}X(\mathbf{\Omega})\sum_{i=0}^{3} G_i(\mathbf{\Omega})F_i(\mathbf{\Omega}) \\
&= \frac{1}{4}X(\mathbf{\Omega})\sum_{i=0}^{3} H(\mathbf{\Omega} + \tilde{\mathbf{k}}_i)H(-\mathbf{\Omega} + \tilde{\mathbf{k}}_i) \\
&= \frac{1}{4}X(\mathbf{\Omega})\sum_{i=0}^{3} |H(\mathbf{\Omega} + \tilde{\mathbf{k}}_i)|^2.
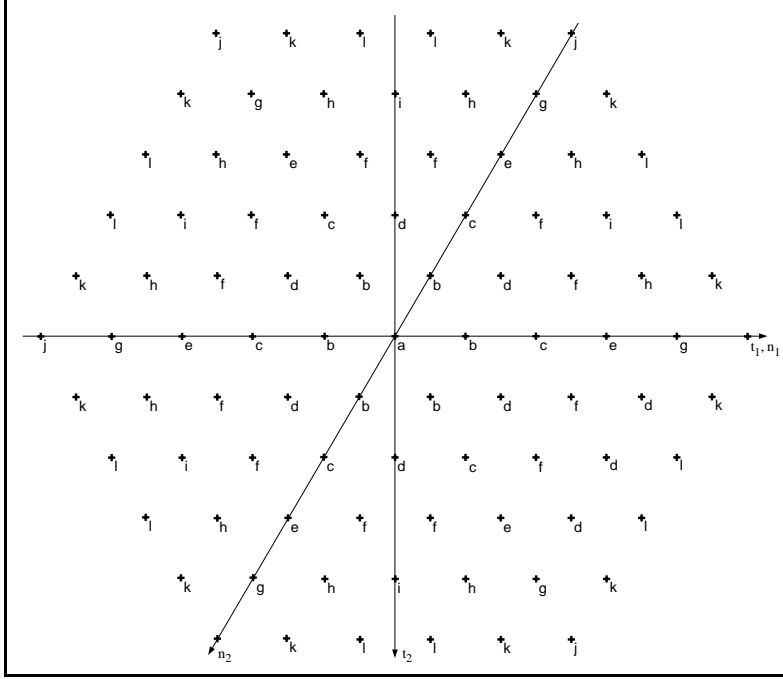\end{aligned}
$$

Fig. 6. Region of support of a 5-ring hexagonally symmetric filter. The parameters $a$ through $l$ refer to the low-pass filter coefficients $h(\mathbf{n})$.

Note that the aliasing cancellation is exact, and independent of the choice of $H(\mathbf{\Omega})$, and the design problem is reduced to finding a filter satisfying the constraint

$$\sum_{i=0}^{3} |H(\mathbf{\Omega} + \tilde{\mathbf{k}}_i)|^2 = 4. \tag{25}$$

A low-pass solution for $H(\mathbf{\Omega})$ in the above equation results in a band-splitting system which may be cascaded hierarchically through the low-pass band of the QMF bank to produce a multiresolution decomposition in two dimensions. Simoncelli [2] describes a simple frequency-sampling design method that produces hexagonally symmetric QMFs with small regions of support for which perfect reconstruction was well approximated. Figure 6 shows the region of support of a 5-ring hexagonally symmetric filter. Notice that the size of the filter is measured in terms of the number of hexagonal rings it contains. The parameters $a$ through $l$ in Figure 6 refer to the filter coefficients of the low-pass solution $h(\mathbf{n})$ computed in [2]. Figure 7(a) shows an idealized diagram of the partition of the frequency domain resulting from a 2-level hexagonal multiresolution decomposition.
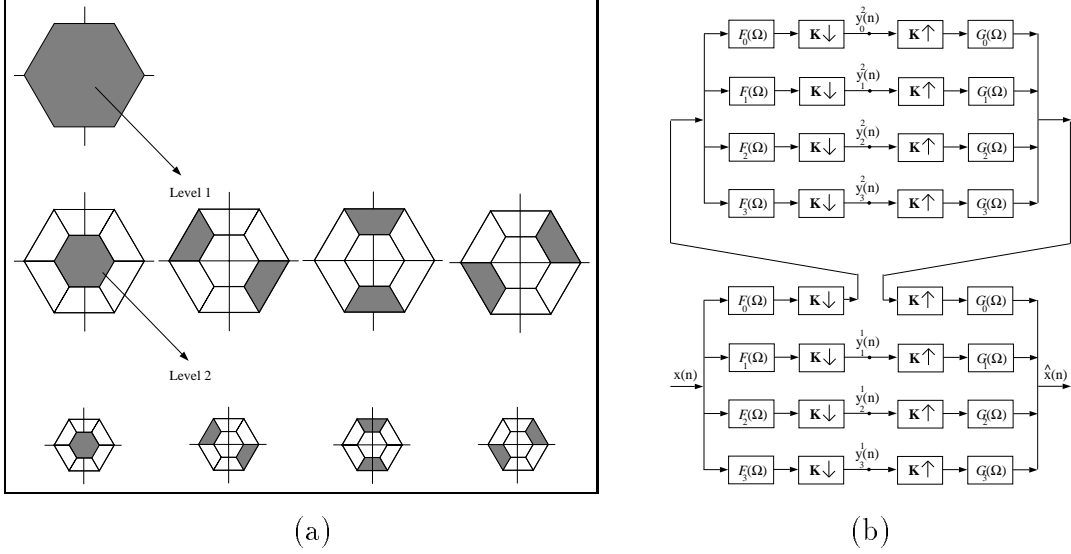
Fig. 7. (a) Partitions of the frequency domain resulting from a 2-level multiresolution decomposition of hexagonal filters. The upper left frequency diagram represents the spectrum of the original image. (b) A two-stage 4-channel analysis/synthesis filter bank.

## D. *Redundant analysis/synthesis filter banks in hexagonal systems*

In this section we discuss the mathematical formulation of redundant analysis/synthesis filter banks in hexagonal systems. In particular, we would like to find equivalent filters for the $i^{th}$ stage of the traditional A/S system shown in Figure 7(b).

It can be easily shown that subsampling by $\mathbf{K}$ followed by filtering with $F_0(\mathbf{\Omega})$ is equivalent to filtering by $F_0(\mathbf{K\Omega})$ followed by subsampling. Hence, the first two steps of low-pass filtering in Figure 7(b) can be replaced by a filter with Fourier transform $F_0(\mathbf{\Omega})F_0(\mathbf{K\Omega})$, followed by subsampling by $\mathbf{K}^2$.

In general, equivalent filters for the $i^{th}$ stage ($i \geq 1$) of a cascade of analysis filters are given by

$$
\begin{aligned}
F_0^i(\mathbf{\Omega}) &= F_0(\mathbf{K}^{i-1}\mathbf{\Omega}) \prod_{l=0}^{i-2} F_0(\mathbf{K}^l\mathbf{\Omega}), \\
F_1^i(\mathbf{\Omega}) &= F_1(\mathbf{K}^{i-1}\mathbf{\Omega}) \prod_{l=0}^{i-2} F_0(\mathbf{K}^l\mathbf{\Omega}), \\
F_2^i(\mathbf{\Omega}) &= F_2(\mathbf{K}^{i-1}\mathbf{\Omega}) \prod_{l=0}^{i-2} F_0(\mathbf{K}^l\mathbf{\Omega}), \\
F_3^i(\mathbf{\Omega}) &= F_3(\mathbf{K}^{i-1}\mathbf{\Omega}) \prod_{l=0}^{i-2} F_0(\mathbf{K}^l\mathbf{\Omega}),
\end{aligned}
\tag{26}
$$

followed by subsampling by $\mathbf{K}^i$. The synthesis filters are obtained in a similar way.
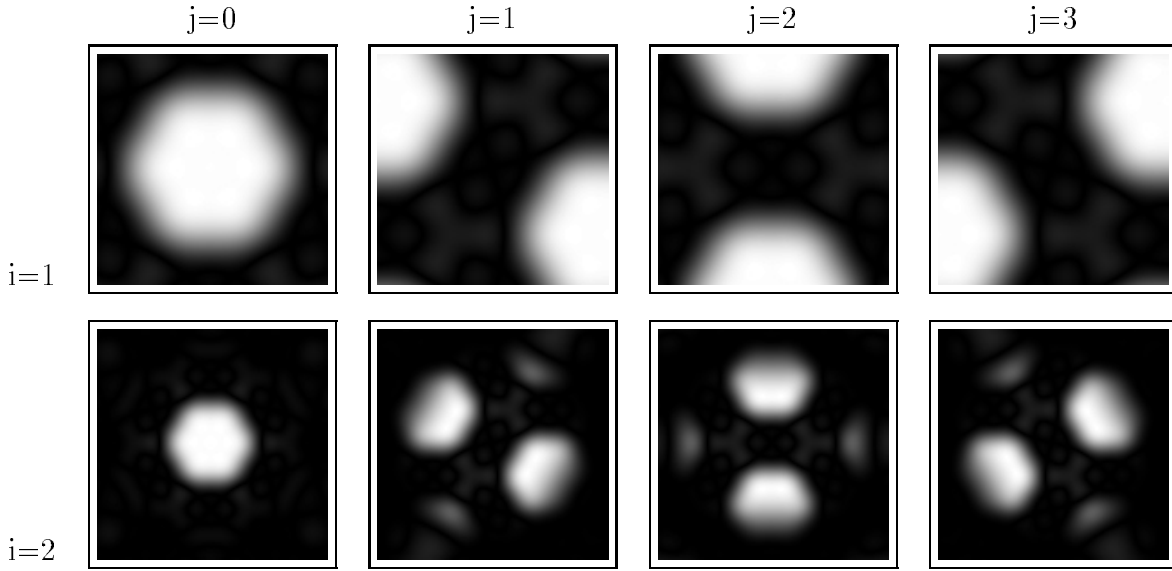
Fig. 8.  Analyzing filters $F_j^i$ for levels 1 and 2.

By removing the operations of down-sampling and up-sampling from the resulting equivalent A/S system we obtain an overcomplete hexagonal multiresolution representation. From Equation (25), perfect reconstruction is also accomplished in this case. Figure 8 shows the magnitude of the equivalent hexagonal filters $F^i$ for levels 1 and 2 for the 4-ring filter coefficients computed in [2].

### E. The discrete Fourier transform in hexagonal systems

Let $\tilde{x}(\mathbf{n})$ be a periodic sequence with periodicity matrix $\mathbf{N}$, that is $\tilde{x}(\mathbf{n}) = \tilde{x}(\mathbf{n} + \mathbf{N}\mathbf{r})$ for any integer vector $\mathbf{r}$. Then it is easy to verify [4] that the following Fourier series relations hold,

$$\tilde{x}(\mathbf{n}) = \frac{1}{|\det \mathbf{N}|} \sum_{\mathbf{k} \in J} \tilde{X}(\mathbf{k}) \exp(j\mathbf{k}^{\mathrm{T}}(2\pi \mathbf{N}^{-1})\mathbf{n}), \tag{27}$$

and,

$$\tilde{X}(\mathbf{k}) = \sum_{\mathbf{n} \in I} \tilde{x}(\mathbf{n}) \exp(-j\mathbf{k}^{\mathrm{T}}(2\pi \mathbf{N}^{-1})\mathbf{n}), \tag{28}$$

where, $I$ and $J$ denote finite-extent regions (consisting of $|\det \mathbf{N}|$ samples) in the $\mathbf{n}$-domain and $\mathbf{k}$-domain, respectively.

Let $x(\mathbf{n})$ be any finite-extent sequence confined to a region $I$ containing $S$ samples. We say that the sequence $x(\mathbf{n})$ admits a periodic extension $\tilde{x}(\mathbf{n})$ with periodicity matrix $\mathbf{N}$ if

$$\tilde{x}(\mathbf{n}) = \tilde{x}(\mathbf{n} + \mathbf{Nr}),$$
$$\tilde{x}(\mathbf{n}) = x(\mathbf{n}), \text{ for } \mathbf{n} \in I,$$

and $S = |\det \mathbf{N}|$.

If $x(\mathbf{n})$ admits a periodic extension with periodicity matrix $\mathbf{N}$ then the Fourier series relation in Equation (28) can be used to define its discrete Fourier transform (DFT) as follows,

$$
\begin{aligned}
\hat{X}(\mathbf{k}) &= \tilde{X}(\mathbf{k}), \ \mathbf{k} \in J, \\
&= \sum_{\mathbf{n} \in I} x(\mathbf{n}) \exp(-j\mathbf{k}^{\mathrm{T}}(2\pi \mathbf{N}^{-1})\mathbf{n}), \ \mathbf{k} \in J.
\end{aligned}
\tag{29}
$$

Similarly, the Fourier series relation in Equation (27) can be used to recover the sequence $x(\mathbf{n})$ from its DFT as follows,

$$
\begin{aligned}
x(\mathbf{n}) &= \tilde{x}(\mathbf{n}), \ \mathbf{n} \in I, \\
&= \frac{1}{|\det \mathbf{N}|} \sum_{\mathbf{k} \in J} \hat{X}(\mathbf{k}) \exp(j\mathbf{k}^{\mathrm{T}}(2\pi \mathbf{N}^{-1})\mathbf{n}), \ \mathbf{n} \in I.
\end{aligned}
\tag{30}
$$

Suppose $x(\mathbf{n})$ is a hexagonally sampled signal with support confined to a region $I$ containing $(2N_1 + N_2)N_2$ samples. In addition suppose that $x(\mathbf{n})$ admits a periodic extension with periodicity matrix

$$
\mathbf{N} = \begin{bmatrix} N_1 + N_2 & N_2 \\ N_2 & 2N_2 \end{bmatrix}.
\tag{31}
$$

Then, we say that $x(\mathbf{n})$ admits a hexagonally periodic extension. Notice that $x(\mathbf{n})$ may admit more than one periodic extension and that each periodic extension defines a different DFT. It is easy to show that the DFT of each admissible periodic extension of $x(\mathbf{n})$ corresponds to a sampled version of its Fourier transform, and that the sampling lattice is controlled through the periodicity matrix $\mathbf{N}$. This result is a consequence of the following relation between the Fourier transform (3) and the discrete Fourier transform (29) of $x(\mathbf{n})$,

$$\hat{X}(\mathbf{k}) = X(\boldsymbol{\omega})\big|_{\boldsymbol{\omega}=2\pi \mathbf{N}^{-\mathrm{T}}\mathbf{k}}.$$

Using the more general definition of the Fourier transform (5) that accounts for the sampling lattice used to sample the original 2-D analog signal we can write

$$\hat{X}(\mathbf{k}) = X_{\mathbf{V}}(\boldsymbol{\Omega})\big|_{\boldsymbol{\Omega}=2\pi(\mathbf{VN})^{-\mathrm{T}}\mathbf{k}}.
\tag{32}$$

It then follows from Equations (31) and (32) that for $N_1 = N_2 = N$, that is, for

$$\mathbf{N} = \begin{bmatrix} 2N & N \\ N & 2N \end{bmatrix}, \tag{33}$$

the DFT of $x(\mathbf{n})$ corresponds to a hexagonal sampled version of its Fourier transform. In this case Equation (29) is referred to as the hexagonal discrete Fourier transform (HDFT) of $x(\mathbf{n})$. It is easy to verify from (29) and (33) that the HDFT of $x(\mathbf{n})$ is given by

$$\begin{aligned}
\hat{X}(k_1, k_2) &= \sum_{(n_1, n_2) \in I} x(n_1, n_2) \exp\left[ -j\frac{2\pi}{3N} \left( (2n_1 - n_2)k_1 + (2n_2 - n_1)k_2 \right) \right], \\
&= \sum_{(n_1, n_2) \in I} x(n_1, n_2) \exp\left[ -j \left( \frac{\pi}{3N}(2n_1 - n_2)(2k_1 - k_2) + \frac{\pi}{N}n_2 k_2 \right) \right].
\end{aligned} \tag{34}$$

Mersereau [4] showed that efficient algorithms for the implementation of the discrete Fourier transform (29) exist if the periodicity matrix $\mathbf{N}$ is composite (i.e., if $\mathbf{N}$ can be factored into a nontrivial product of integer matrices.) For $N = 2^l$, $l \geq 0$ we observe that the periodicity matrix $\mathbf{N}$ in (33) can be factored as,

$$\mathbf{N} = \begin{bmatrix} 2 & 1 \\ 1 & 2 \end{bmatrix} \begin{bmatrix} 2 & 0 \\ 0 & 2 \end{bmatrix}^l. \tag{35}$$

This factorization leads to an efficient implementation of (34) known as the hexagonal fast Fourier transform (HFFT). Implementation details of the HFFT can be found in [1].

## II. Implementation

Next, we present implementation details of hexagonal multiresolution representations. Section II-A describes the selection of image support for efficient signal processing with hexagonal systems. Section II-B describes filtering in hexagonal sampling systems using a HFFT based strategy and the computation of hexagonal multiresolution representations. Finally, Section II-C describes the computation of overcomplete hexagonal multiresolution representations. A listing of MATLAB functions implementing hexagonal multiresolution representations is available at http://www.iprg.cise.ufl.edu/.

### A. Image support in hexagonal systems

Efficient discrete signal processing in hexagonal sampling systems can be achieved by using the hexagonal fast Fourier transform but at the cost of restricting sequences to

those that admit a hexagonally periodic extension with $N_1 = N_2 = N$ and $N = 2^l$, $l \geq 0$. Systematic application of the HFFT to image processing further restricts sequences to rectangular regions. It is easy to verify that for any $N = 2^l$, $l \geq 1$ it is possible to find a rectangular region $I_l$ such that any sequence with support confined to $I_l$ admits a hexagonally periodic extension. Figure 9 shows such a sequence confined to region $I_1$ and its hexagonally periodic extension. For any $l \geq 1$, region $I_{l+1}$ may be obtained from $I_l$ by doubling the number of rows and the number of samples per rows in $I_l$. Notice that given the periodic sequence shown in Figure 9 there exists more than one fundamental period such that when extended periodically in a hexagonal fashion results in the same periodic sequence. In particular, Figure 9 shows a parallelogram $P_1$ containing an alternative set of samples that could be used to define the same periodic sequence but greatly simplifies the HFFT computation. The simplification comes from the fact that samples contained in the parallelogram can be stored in an array of size $N \times 3N$ where the indices of the array directly correspond to the coordinates $(n_1, n_2)$ of the samples. It is straight forward to verify that for any sequence confined to $I_l$, $l \geq 1$ there exists a parallelogram $P_l$ containing an alternative set of samples that defines the same periodic sequence. For any $l \geq 1$, $P_{l+1}$ is obtained from $P_l$ in the same way $I_{l+1}$ was obtained from $I_l$. It follows that computation of the HFFT for a sequence confined to $I_l$ can be accomplished by using Equation (34) where $I$ corresponds to a region defined by $P_l$.

Although there are certain image processing applications in which image samples are acquired in a hexagonal fashion, most digital detectors (e.g., CCDs) sample images rectangularly with the same sampling rate along both directions. Processing a rectangularly sampled image with a hexagonal sampling system requires that the rectangularly sampled image be mapped into a hexagonal sampling lattice [3], [2]. For square images whose size is a power of two we describe a strategy that maps a rectangularly sampled image confined to a square region consisting of $2N \times 2N$ samples ($N = 2^l$, $l \geq 1$) into a hexagonally sampled image confined to a rectangular region for which it is possible to compute its HFFT. This mapping may be accomplished in two distinct ways. If the original image is oversampled, we first interpolate horizontally by a factor of 3 and then mask the result with the masking function $M_1(n_h, n_v) = \frac{1}{4}(1 + (-1)^{n_h})(1 + (-1)^{n_h/2 + n_v})$ as shown in Figure 10. The resulting
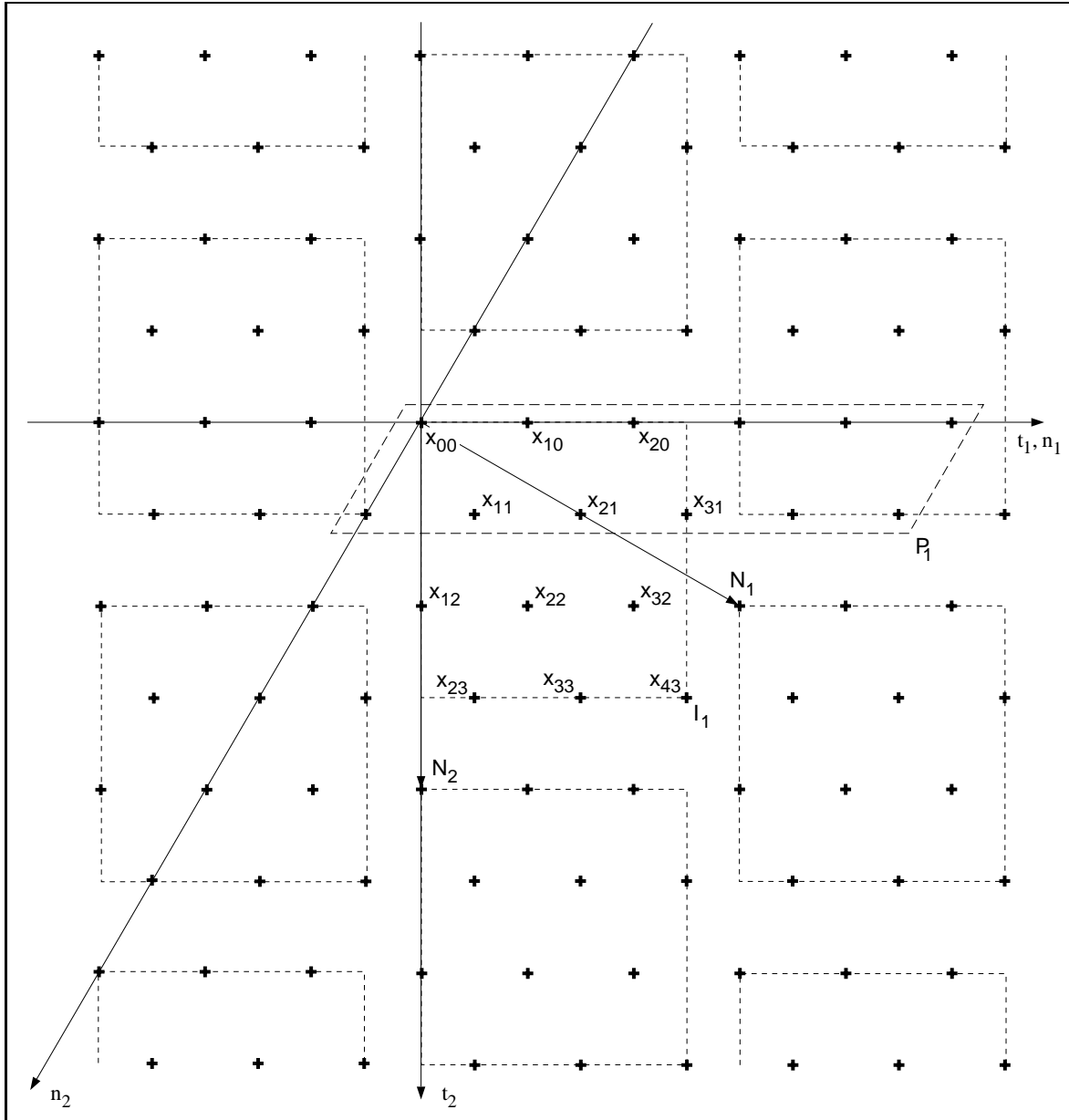
Fig. 9. Hexagonally sampled sequence confined to a rectangular region $I_1$ and its hexagonally periodic extension. Parallelogram $P_1$ contains an alternative set of samples that defines the same periodic sequence.
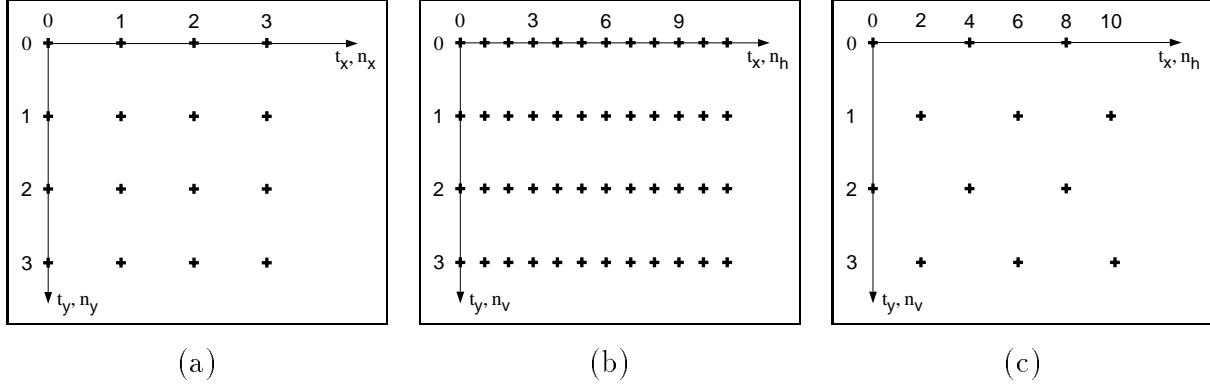
Fig. 10. Mapping a rectangularly sampled image into a hexagonal sampling lattice. (a) Rectangular lattice, (b) Intermediate lattice with interpolated samples, (c) Sampling function.
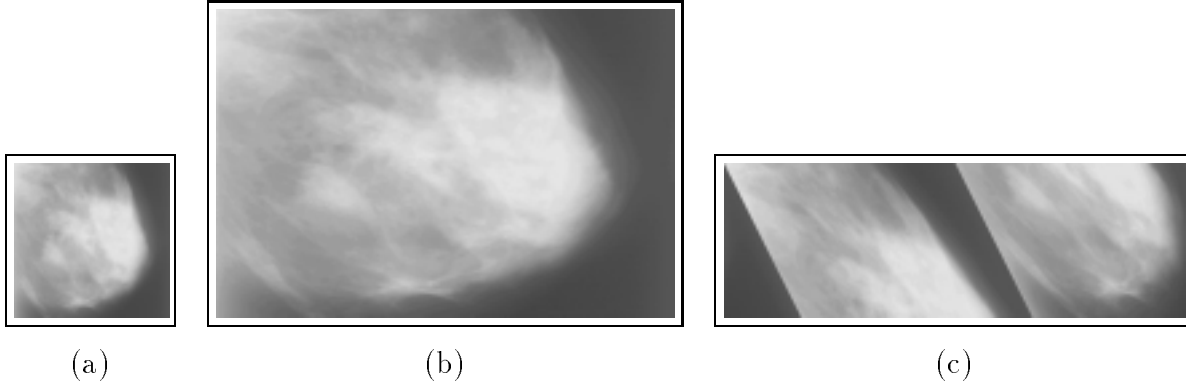


Fig. 11. (a) A $512 \times 512$ rectangularly sampled radiograph of the breast, (b) Image with interpolated samples, (c) Hexagonally sampled image confined to $P_9$ – Axes $n_1$ and $n_2$ are shown at 90 degrees.

image is confined to region $I_l$ and consists of $3N^2$ samples (25% fewer samples than the original). In this case, it is assumed that oversampling of the original image accounts for the reduction of the number of samples in the resulting image. Alternatively, if the original image is critically sampled, we interpolate horizontally by a factor of 3 and vertically by a factor of 2 and mask the result with the masking function $M_2(n_h, n_v) = \frac{1}{2}(1 + (-1)^{n_h + n_v})$. In this case the resulting image is confined to region $I_{l+1}$ and consists of $3(2N)^2$ samples. In each case the resulting sampling lattice gives a reasonable geometric *approximation* to a hexagonal sampling lattice. Note that the oversampled method or the critically sampled method, together with the equivalence between $I_l$ and $P_l$ can be used to map a $2N \times 2N$ rectangularly sampled image into $P_l$ or $P_{l+1}$, respectively. Figure 11 shows a $512 \times 512$ rectangularly sampled image and its mapping into $P_9$ using the critically sampled strategy described above.
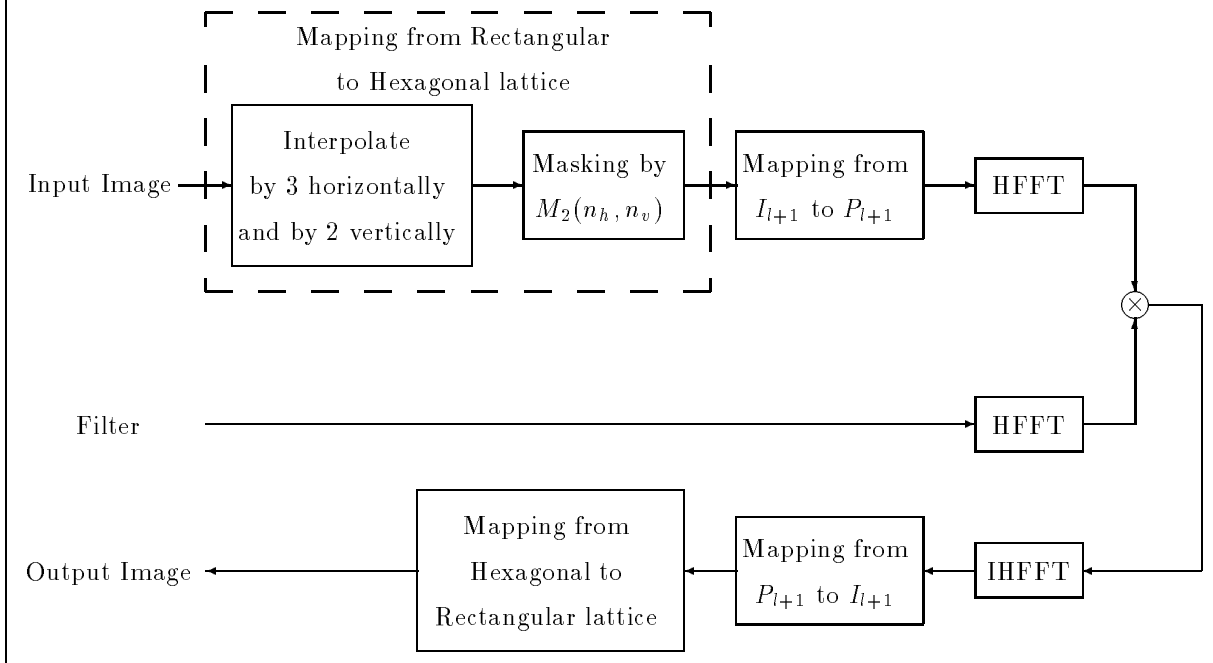
Fig. 12. Filtering a rectangularly sampled image of size $2N \times 2N$, $N = 2^l$ with a hexagonally sampled system by means of the HFFT. Critically sampled case shown.

## B. Multiresolution representations in hexagonal systems

Filtering an image with a hexagonal filter may be accomplished by computing the product of the HFFTs of the image and the filter kernel and taking the inverse hexagonal fast Fourier transform (IHFFT) of the result. This approach requires that both the image and the filter kernel be supported in the same region $I_l$. Again, computation of the HFFT can be accomplished using $P_l$ instead of $I_l$ due to periodicity. Figure 12 shows a block diagram of the filtering process described above for a rectangularly sampled signal confined to a square region of size $2N \times 2N$, $N = 2^l$.

Here, we are interested in filtering an image with the quadrature mirror filters in equation (23) given the low-pass solution $h(n_1, n_2)$ computed in [2]. Replacing equations (22) and (24) in (23) and using relations (5) and (32) we obtain the following HDFT relations for

the filters,

$$
\begin{aligned}
\hat{F}_0(\mathbf{k}) &= \hat{G}_0(-\mathbf{k}) &= \sum_{\mathbf{n} \in I} h_0(\mathbf{n}) \exp(-j\mathbf{k}^T(2\pi\mathbf{N}^{-1})\mathbf{n}), \\
\hat{F}_1(\mathbf{k}) &= \hat{G}_1(-\mathbf{k}) &= \exp\left(j\frac{2\pi}{3N}(2k_1 - k_2)\right) \sum_{\mathbf{n} \in I} h_1(\mathbf{n}) \exp(-j\mathbf{k}^T(2\pi\mathbf{N}^{-1})\mathbf{n}), \\
\hat{F}_2(\mathbf{k}) &= \hat{G}_2(-\mathbf{k}) &= \exp\left(j\frac{2\pi}{3N}(k_1 + k_2)\right) \sum_{\mathbf{n} \in I} h_2(\mathbf{n}) \exp(-j\mathbf{k}^T(2\pi\mathbf{N}^{-1})\mathbf{n}), \\
\hat{F}_3(\mathbf{k}) &= \hat{G}_3(-\mathbf{k}) &= \exp\left(j\frac{2\pi}{3N}(k_1 - 2k_2)\right) \sum_{\mathbf{n} \in I} h_3(\mathbf{n}) \exp(-j\mathbf{k}^T(2\pi\mathbf{N}^{-1})\mathbf{n}),
\end{aligned}
\tag{36}
$$

where $h_0(\mathbf{n}) = h(n_1, n_2)$, $h_1(\mathbf{n}) = (-1)^{n_1} h(n_1, n_2)$, $h_2(\mathbf{n}) = (-1)^{n_2} h(n_1, n_2)$, $h_3(\mathbf{n}) = (-1)^{n_1 + n_2} h(n_1, n_2)$, and $I$ is the region of support of the filter kernels. It follows from the equations above that the HFFT of filters $f_k(\mathbf{n})$ can be obtained by modulating the HFFTs of the kernels $h_k(\mathbf{n})$ with complex exponentials. Notice that filtering an image confined to a region $I_l$ with an $r$-ring filter kernel $f_k(\mathbf{n})$ using the HFFT-filtering strategy described above requires that the region of support of the kernel be confined to $I_l$ (or equivalently to $P_l$). Indeed, this requirement is satisfied as long as $l \geq \lceil \log_2(2r + 1) \rceil - 1$.

A one-level multiresolution decomposition of an image can be obtained by filtering the image with the filters kernels $f_k(\mathbf{n})$ followed by down-sampling (as shown in Figure 5.) This can be accomplished using the HFFT-filtering strategy described above if the image is confined to $I_l$ or $P_l$. Notice that if we work with sequences confined to $P_l$ then the down-sampling operation is equivalent to taking every other row and every other column of the array storing the sequence. An $(L + 1)$-level multiresolution decomposition can then be obtained recursively by cascading an analysis section through the low-pass branch of an $L$-level multiresolution decomposition. Notice that the maximum number of levels is limited by the smallest $P_l$ supporting the filter kernels. Figure 13 shows a two-level hexagonal multiresolution decomposition and reconstruction using the 3-ring low-pass solution to (23) computed in [2]. An algorithm for the multiresolution reconstruction follows directly from its decomposition.

## C. Overcomplete multiresolution representations in hexagonal systems

An overcomplete hexagonal multiresolution representation is computed by filtering an image with the equivalent filters introduced in Section I-D. Using the HFFT-filtering strategy described previously it follows that the equivalent filters $F_k^i$ can be computed
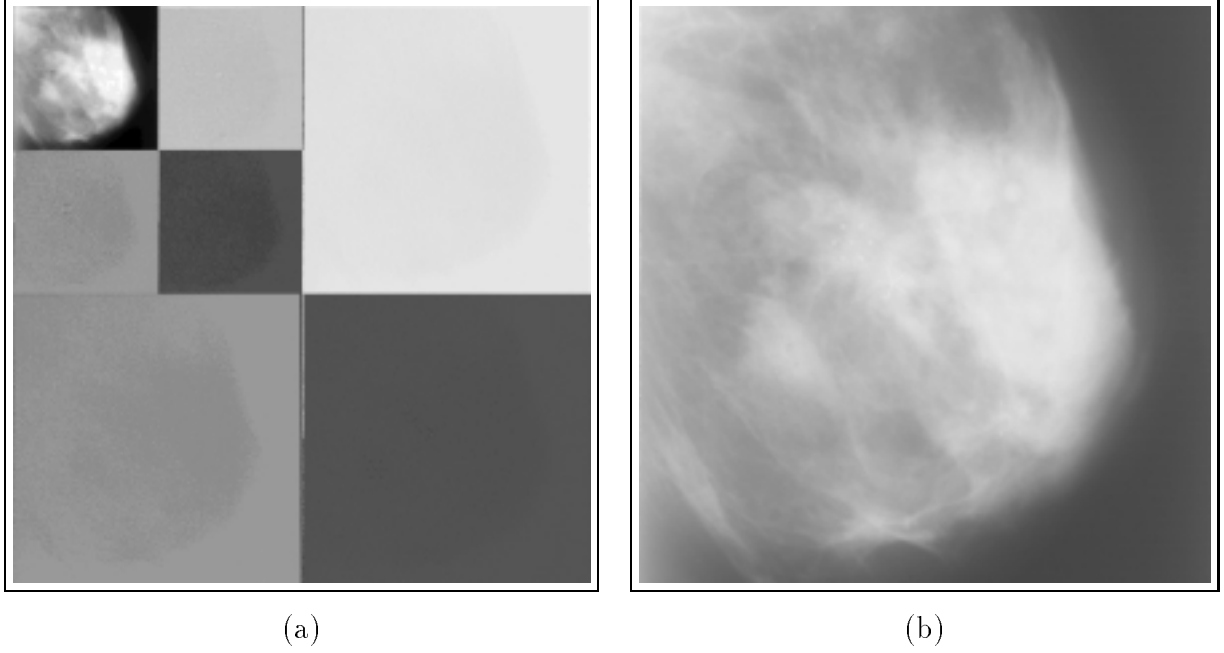
(a)                 (b)

Fig. 13. Two-level hexagonal multiresolution representation. (a) Decomposition. (b) Reconstruction. Both images are displayed on their original sampling lattice.

taking the product of the HFFTs of filter kernels $f_{k,l}(\mathbf{n})$ where $F_{k,l}(\mathbf{\Omega}) = F_k(\mathbf{K}^l\mathbf{\Omega})$. It is easy to show that the following HDFT relation holds for $f_{k,l}(\mathbf{n})$,

$$\hat{F}_{k,l}(\mathbf{k}) = \hat{F}_k(\mathbf{K}^l\mathbf{k}).$$

This result combined with equation (36) leads to the following HDFT relations for the filters,

$$
\begin{aligned}
\hat{F}_{0,l}(\mathbf{k}) &= \hat{G}_{0,l}(-\mathbf{k}) &= \sum_{\mathbf{n}\in I} h_{0,l}(\mathbf{n}) \exp(-j\mathbf{k}^{\mathrm{T}}(2\pi\mathbf{N}^{-1})\mathbf{n}), \\
\hat{F}_{1,l}(\mathbf{k}) &= \hat{G}_{1,l}(-\mathbf{k}) &= \exp\left(j\frac{2^{l+1}\pi}{3N}(2k_1 - k_2)\right) \sum_{\mathbf{n}\in I} h_{1,l}(\mathbf{n}) \exp(-j\mathbf{k}^{\mathrm{T}}(2\pi\mathbf{N}^{-1})\mathbf{n}), \\
\hat{F}_{2,l}(\mathbf{k}) &= \hat{G}_{2,l}(-\mathbf{k}) &= \exp\left(j\frac{2^{l+1}\pi}{3N}(k_1 + k_2)\right) \sum_{\mathbf{n}\in I} h_{2,l}(\mathbf{n}) \exp(-j\mathbf{k}^{\mathrm{T}}(2\pi\mathbf{N}^{-1})\mathbf{n}), \\
\hat{F}_{3,l}(\mathbf{k}) &= \hat{G}_{3,l}(-\mathbf{k}) &= \exp\left(j\frac{2^{l+1}\pi}{3N}(k_1 - 2k_2)\right) \sum_{\mathbf{n}\in I} h_{3,l}(\mathbf{n}) \exp(-j\mathbf{k}^{\mathrm{T}}(2\pi\mathbf{N}^{-1})\mathbf{n}),
\end{aligned}
\tag{37}
$$

where

$$
h_{k,l}(\mathbf{n}) = \begin{cases} h\left((\mathbf{K}^l)^{-1}\mathbf{n}\right), & \text{if } (\mathbf{K}^l)^{-1}\mathbf{n} \text{ is an integer vector,} \\ 0, & \text{otherwise.} \end{cases}
$$

Note that in the above derivation we used the fact that $\mathbf{K}$ defined a separable subsampling matrix. It follows from the equation above that the HFFT of the filter kernels $f_{k,l}(\mathbf{n})$ can be obtained by modulating the HFFTs of the kernels $h_{k,l}(\mathbf{n})$ with complex exponentials. The filters $h_{k,l}(\mathbf{n})$ can be constructed by up-sampling $h_k(\mathbf{n})$ with sampling matrix $\mathbf{K}^l$. The filters $F_k^i$ can then be computed following equation (26) with the filters given in (37). Notice that it is possible to discard the complex exponentials and still obtain perfect reconstruction. However, this will define a different set of filters. A hexagonal overcomplete multiresolution representation of an image can be obtained by filtering the image with the filters $f_k^i$ derived above. Figure 14 shows an example of hexagonal overcomplete multiresolution representations applied to a digitized radiograph of the breast. Contrast enhancement was accomplished adaptively based on the location of multiscale edges derived from the hexagonal overcomplete multiresolution representation. Figure 15 shows another example of this technique applied to a region of interest of a digitized radiograph of the chest. Please refer to [8] for a complete description of this enhancement algorithm and other possible methods of enhancement.

(a)                                                                (b)





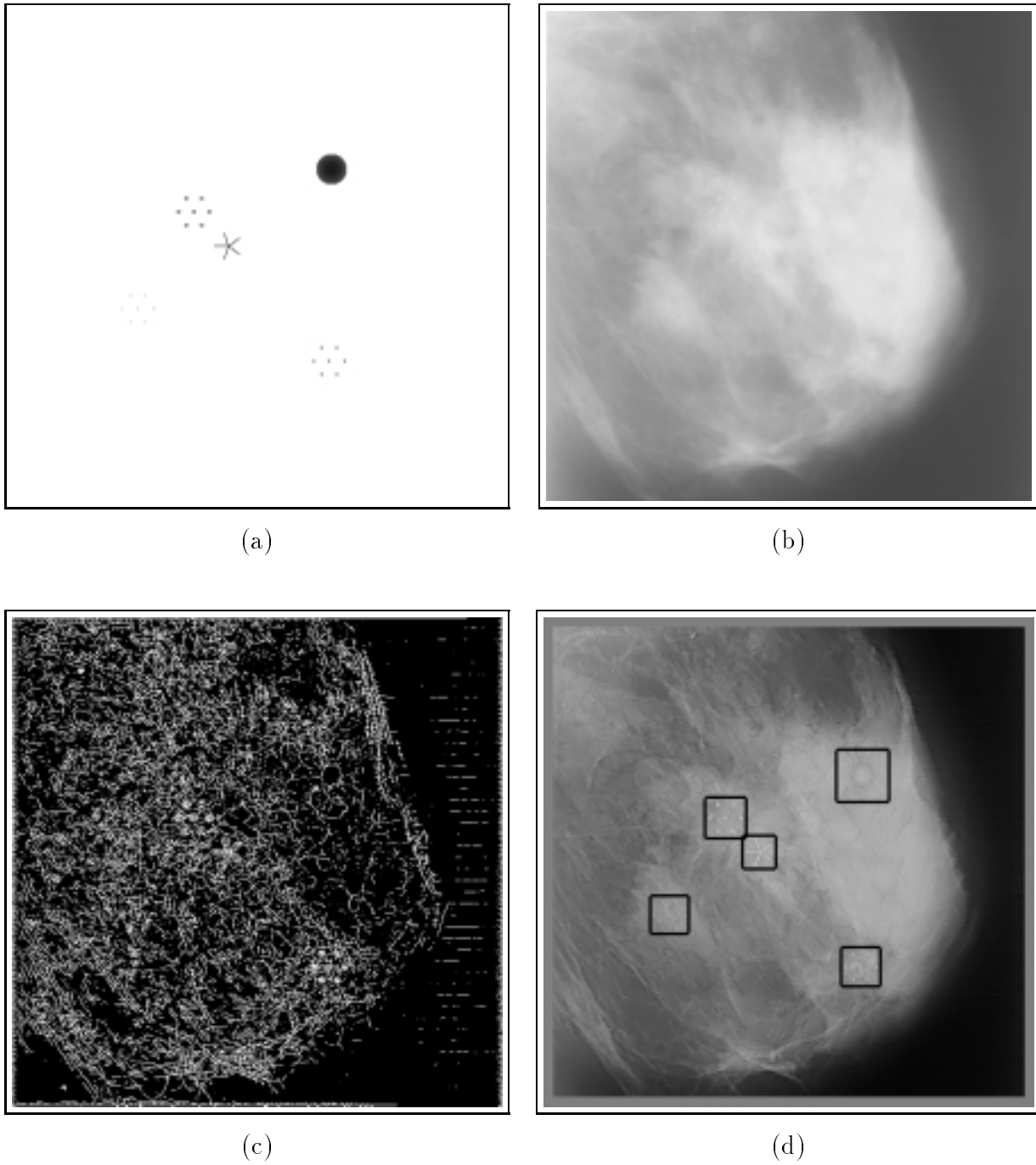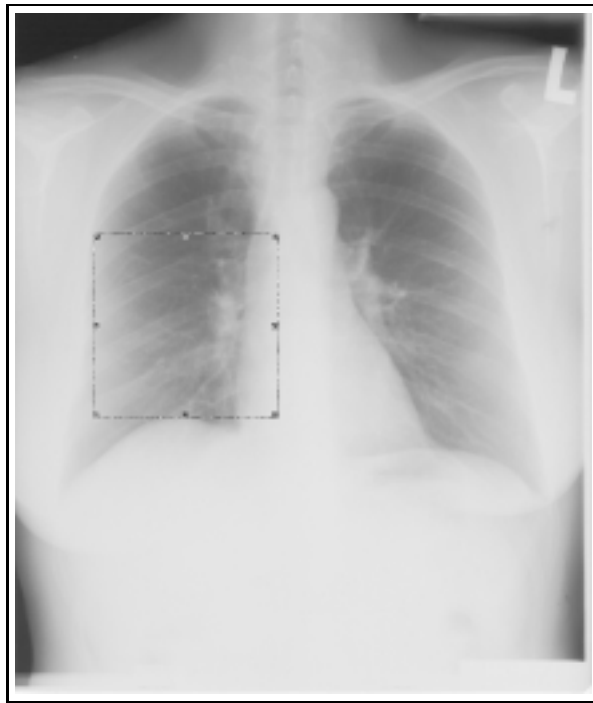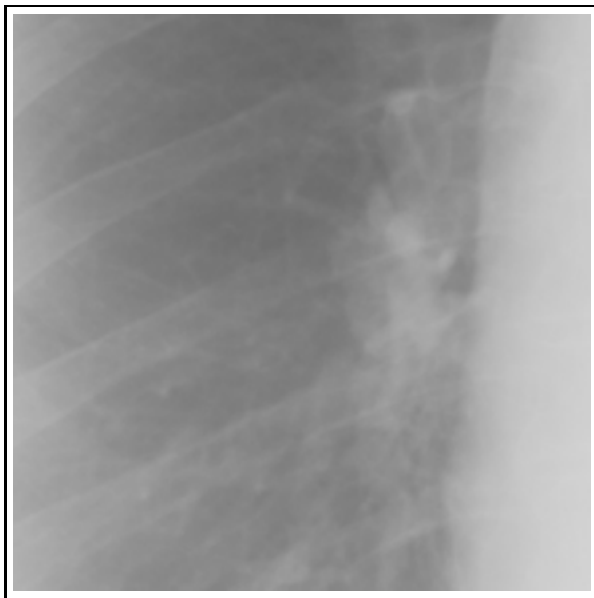(c)                                                                (d)

Fig. 14.  (a) Mathematical phantom. (b) Mammogram blended with phantom. (c) Combined orientations of hexagonal edges obtained from level 3 coefficients. (d) Contrast enhancement by multiscale edges obtained from a hexagonal overcomplete multiresolution representation.

(a)



(b)



(c)

Fig. 15. (a) Original image. (b) Region of interest. (c) Enhanced region of interest via multiscale analysis.

# REFERENCES

[1] R.M. Mersereau, "The processing of hexagonally sampled two-dimensional signals", *Proceedings of the IEEE*, vol. 67, no. 6, pp. 930–949, June 1979.

[2] E.P. Simoncelli and E.H. Adelson, "Non-separable extensions of quadrature mirror filters to multiple dimensions", *Proceedings of the IEEE*, vol. 78, no. 4, pp. 652–663, Apr. 1990.

[3] R.M. Mersereau and T.C. Speake, "The processing of periodically sampled multidimensional signals", *IEEE Transactions on Acoustics, Speech, and Signal Processing*, vol. 31, no. 1, pp. 188–194, Feb. 1983.

[4] R.M. Mersereau and D.E. Dudgeon, *Multidimensional Digital Signal Processing*, Prentice-Hall, Inc., Englewood Cliffs, New Jersey, 1984.

[5] E. Viscito and J.P. Allebach, "The analysis and design of multidimensional fir perfect reconstruction filter banks for arbitrary sampling lattices", *IEEE Transactions on Circuits and Systems*, vol. 38, no. 1, pp. 29–41, Jan. 1981.

[6] A. Laine and S. Schuler, "Hexagonal wavelet processing of digital mammography", in *Medical Imaging 1993*, Newport Beach, California, Feb. 1993, Part of SPIE's Thematic Applied Science and Engineering Series.

[7] M. Newman, *Integral Matrices*, Academic Press, New York, 1972.

[8] A. Laine, S. Schuler, J. Fan, and W. Huda, "Mammographic feature enhancement by multiscale analysis", *IEEE Transaction on Medical Imaging*, vol. 13, no. 4, pp. 725–740, Dec. 1994.